

Improvement of Electrochemical Performance of LiMn_2O_4 Composite Cathode by ox-MWCNT addition for Li-ion Battery

Su-qin Liu,* Jian-feng Zhang, Ke-long Huang and Jin-gang Yu

College of Chemistry & Chemical Engineering, Central South University, Changsha 410083, P. R. China

Nanotubos de carbono de multi-paredes oxidados (ox-MWCNT) foram utilizados como condutores adicionais para preparar uma nova rede de cátodos para bateria de íons de lítio. A morfologia foi analisada pelo microscópio de varredura eletrônico, e partículas ativas de LiMn_2O_4 foram ligadas ao ox-MWCNT com a formação da rede tridimensional de fiação. O transporte de elétrons e a atividade eletroquímica foram melhorados de forma eficaz. Testes galvanostáticos de carga-descarga do cátodo $\text{LiMn}_2\text{O}_4/\text{ox-MWCNT}$ mostrou que a capacidade de descarga inicial são 119,4, 110,6, 105,5 e 91,4 mAh g^{-1} à taxa de 0,1, 0,5, 1 e 2 C, respectivamente, os quais são muito superiores aos de $\text{LiMn}_2\text{O}_4/\text{acetileno}$ (AB), de mesmo conteúdo. A espectroscopia da impedância eletroquímica AC mostrou que a resistência da transferência de carga (R_{ct}) do eletrodo composto reduziu de 34,32 Ω para $\text{LiMn}_2\text{O}_4/\text{ox-MWCNT}$, em comparação ao valor de 53,2 Ω para $\text{LiMn}_2\text{O}_4/\text{AB}$. De um modo geral, se verificou que uma rede condutora para facilitar a transferência de elétrons e fazer uma boa conexão das partícula ativas com o material da rede desempenham um papel importante para avaliar a capacidade e eficiência do ciclo.

Oxidized multi-walled carbon nanotubes (ox-MWCNT) were used as conducting addition to prepare a novel network composite cathode for lithium ion battery. The morphology was analyzed by scanning electron microscope, LiMn_2O_4 active particles were connected by ox-MWCNT with the formation of three-dimensional networking wiring. Electron transport and electrochemical activity were improved effectively. Galvanostatic charge-discharge tests of $\text{LiMn}_2\text{O}_4/\text{ox-MWCNT}$ cathode showed that the initial discharge capacities are 119.4, 110.6, 105.5 and 91.4 mAh g^{-1} at the rate of 0.1, 0.5, 1 and 2 C, respectively, which were much higher than $\text{LiMn}_2\text{O}_4/\text{acetylene black}$ (AB) at the same content. The electrochemical AC impedance spectroscopy showed that the charge transfer resistance (R_{ct}) of the composite electrode reduced obviously contrasting to 34.32 Ω for $\text{LiMn}_2\text{O}_4/\text{ox-MWCNT}$ and 53.2 Ω for $\text{LiMn}_2\text{O}_4/\text{AB}$. Overall, it is found that a conductive network to facilitate electron transfer and good connection of the active-material particle to the network were playing an important role to rate capability and cycle efficiency.

Keywords: oxidized multi-walled carbon nanotubes, composite electrode, conducting network, lithium ion batteries

Introduction

Among several materials under development for use as cathode in lithium ion battery, LiMn_2O_4 appears to be a promising candidate because of its low cost, low toxicity, environmentally benign nature and has a good thermal behavior, which does not require additional expensive safety devices.¹⁻³

In the working mechanism of lithium ion battery, electron exchange is accompanied simultaneously in the process of lithium ion de/intercalation. Therefore the

high lithium ion and electron conductivity are essential to the good performance of LiMn_2O_4 electrode. Thus, an electronically conductive phase, such as carbon black or acetylene black, may be necessary in order to form composite electrode with adequate electronic conductivity.^{4,5} As a conventional conductive additive, 5-20% of acetylene black is added in cathode material.⁶⁻⁸ Furthermore, carbon-fiber coating⁹ and metallic particles addition¹⁰ were used to enhance electron conducting. Multi-walled carbon nanotubes (MWCNTs) have many advantages over amorphous acetylene black, such as high conductivity, tubular shape and large aspect ratio. Moreover, MWCNTs can connect cathode active particles to form a

*e-mail: sqliu2003@126.com

conductive networking wiring. Yang *et al.*^{11,12} reported that electron conductivity of MWCNTs thin film was around $(1-4) \times 10^2 \text{ S cm}^{-1}$ along the nanotube axis and $5-25 \text{ S cm}^{-1}$ perpendicular to the axis, respectively. Whittingham *et al.*¹³ successfully increased the conductivity of LiFePO_4 cathode by adding MWCNTs using hydrothermal method. Here, we demonstrate that $\text{LiMn}_2\text{O}_4/\text{ox-MWCNT}$ composite cathode could improve electronic conducting and rate capability. Moreover, kinetic of Li-ion de/intercalation from composite cathode is also studied.

Experimental

LiMn_2O_4 was prepared from stoichiometric amount of LiNO_3 and Electrolytic Manganese Dioxide (EMD) by a conventional solid-state reaction. The mixture was ground homogeneously in an agate mortar, preheated at 450°C for 6 h and at 750°C for 20 h in muffle in succession. After being cooled to room temperature, the final product was obtained.

Ox-MWCNT (Oxidized MWCNTs) were prepared as follows: approximately 80 mg of a purified sample of MWCNTs were refluxed in 50 mL of 70% HNO_3 at 80°C for 10 h and sonicated for 30 min, stirred for 24 h. The solid was collected on a 100 nm pore membrane and then washed with distilled water until the pH value of the filtrate reached 7.0. Prior to measurements and cathode preparation, acetylene black and ox-MWCNT were heated at 120°C for 12 h under vacuum to remove surface-adsorbed species, such as H_2O and hydrocarbons.

Phase structure of LiMn_2O_4 was analyzed by powder X-ray diffraction (XRD) using Rigaku D/max-2550VB with CuK_α radiation. The scanning rate was 4° min^{-1} and the scanning range was from $15^\circ-80^\circ$. Morphologies of the composite cathode were observed by scanning electron microscope (SEM) using JSM25600LV. FT-IR spectroscopy was measured by Nicolet 7000-C with 4 cm^{-1} resolution. The four-point probe direct current method was used to measure the electronic conductivity at room temperature using a CMT-SR2000N (Mission Peak Optics Inc.).

The cathode slurry was prepared by mixing LiMn_2O_4 , polytetrafluoroethylene (PTFE) and acetylene black or ox-MWCNT in the weight ratio of 90:5:5 in N-methyl-2-pyrrolidone (NMP) solvent. The slurry was coated onto a 1 cm^2 stainless steel current collector. The electrode were dried for 12 h in a vacuum oven at 120°C then pressed at 20 MPa. A two electrode cell composed of a working electrode and lithium foil as the anode, was assembled in an Ar filled glove box with less than 1ppm each of oxygen and moisture. The electrolyte was a 1 mol L^{-1} LiPF_6 solution of 1:1:1 (v/v/v in volume) of ethylene carbonate(EC) diethyl

carbonate(DEC) and ethyl methyl carbon(EMC). These cells were charge-discharged galvanostatically on LAND 2001CT battery tester (Wuhan, P.R. China) at cutoff voltage between 3.2 and 4.3 V. EIS was performed from 10 mHz to 100 kHz frequency range using Zahner elektrik (IM6) by applying an ac voltage of 5 mV amplitude.

Results and Discussion

The powder X-ray diffraction pattern of LiMn_2O_4 prepared by solid state reaction is presented in Figure 1. The crystal parameter can be measured to be $a = 8.221 \text{ \AA}$, which is close to that of stoichiometric LiMn_2O_4 spinel (8.245 \AA).¹⁴

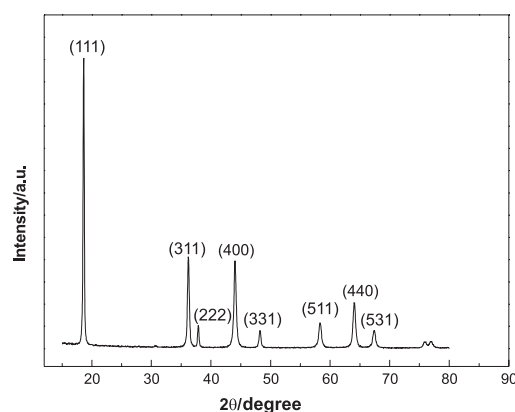


Figure 1. XRD pattern of sample LiMn_2O_4 synthesized by solid state reactions.

Figure 2 (a) shows that acetylene black is discrete and conglomerates in the internal space among active particles. As shown in Figure 2 (b), ox-MWCNT interlace all the particles together to form a network wiring and disperse uniformly in series on the surface of LiMn_2O_4 particles. The electron conducting on the interface between cathode active material and current collector could be improved effectively when ox-MWCNT acted as a conducting bridge. Figure 3 shows the IR spectra of pristine MWCNT and ox-MWCNT. After treatment of pristine MWCNT, we found a peak around 1210 cm^{-1} , but it does not yet have a clear assignment. The peak at 1720 cm^{-1} can be inferred as $\text{C}=\text{O}$ stretching vibration in the COOH group of ox-MWCNT which means that the acid treatment will introduce some $\text{C}=\text{O}$ groups to the end or the side of MWCNT.¹⁵

Figure 4 (a) and (b) presents the initial charge-discharge curves of $\text{LiMn}_2\text{O}_4/\text{ox-MWCNT}$ and $\text{LiMn}_2\text{O}_4/\text{AB}$ composite cathodes with 5 wt.% content at different rates. For $\text{LiMn}_2\text{O}_4/\text{ox-MWCNT}$ composite cathode, at the cutoff voltage between 3.2 and 4.3 V, the discharge capacity is 119.4 mAh g^{-1} at C/10 rate in the first cycle and the coulomb efficiency is 92.6%. The composite cathode

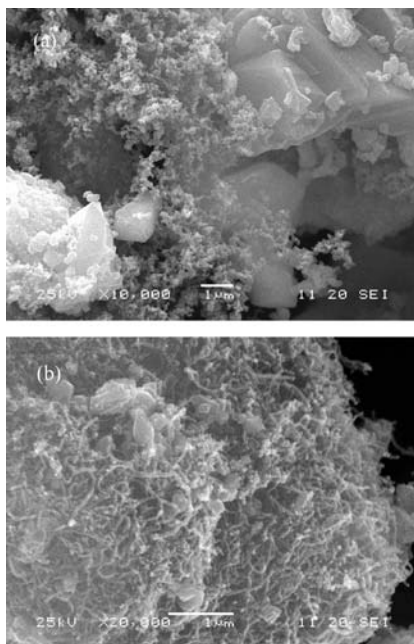


Figure 2. Scanning electron micrographs of the composite cathode of LiMn_2O_4 with (a) acetylene black and (b) ox-MWCNT wiring at the same weight ratio of 5 wt. %.

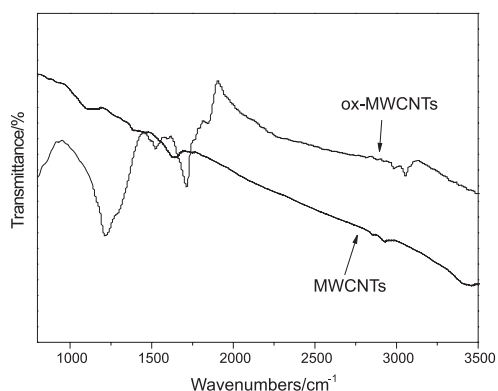


Figure 3. IR spectra of pristine MWCNT and ox-MWCNT.

delivered 110.6, 105.5 and 91.4 mAh g^{-1} when discharged rate were 0.5, 1 and 2 C, respectively. As for $\text{LiMn}_2\text{O}_4/\text{AB}$ composite cathode according to Figure 4(b), the initial discharge capacities were 109.9, 103.4, 94.1 and 80.4 mAh g^{-1} , respectively, which were much lower than that $\text{LiMn}_2\text{O}_4/\text{ox-MWCNT}$ cathode. Son *et al.*¹⁶ reported that Ag nano-particle coated LiMn_2O_4 delivered 96 mAh g^{-1} at 2 C rate when 3.2 wt. % Ag was used. The reasons that the $\text{LiMn}_2\text{O}_4/\text{ox-MWCNT}$ cathode showed an excellent performance were as follows: The conductive network wiring by ox-MWCNT enhanced transport rate of the lithium ions and electrons into the active material. The electrical connections among LiMn_2O_4 particles also enhanced so that the diffusion of lithium ions in the solid state and the electrochemical activity can be improved.

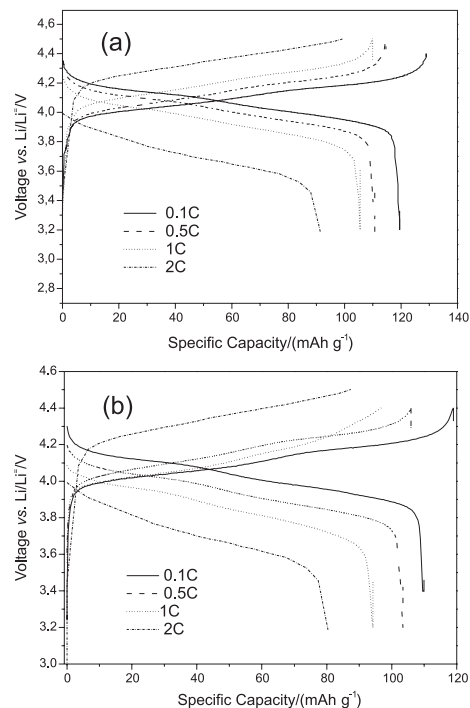


Figure 4. The initial charge-discharge curves of the composite with (a) ox-MWCNT wiring and (b) acetylene black at different rates with the cutoff voltage between 3.2 and 4.3 V.

Furthermore, ox-MWCNT can inhibit irreversible reactions and improve cycle efficiency due to the functional groups on the surface.

Figure 5 presents the cycling performance of LiMn_2O_4 composite cathode mixed with ox-MWCNT or acetylene black at the same content. There is even no evident capacity fading of ox-MWCNT-cathode at 2 C rate, whose capacity retention is 98% after 40 cycles. These results show that ox-MWCNT wiring can improve cycle efficiency and rate capability more effectively than acetylene black. Mukai *et al.*¹⁷ suggested that the a variety of oxo-functional groups and micro-pores might exist on the surface of acetylene black, which resulted in irreversible reactions with electrolytes. Sastry and coworkers¹⁸ have shown that the shape of the conductive material has a substantial effect on the conductivity of the network formed. The contact of active material and the current collector could be enhanced by the three-dimensional network formed by ox-MWCNT, which could prevent irreversible reactions due to deletion of oxide groups. Moreover, ox-MWCNT has low resistance and can enhance the surface intercalation of lithium ions, reducing cell polarization. However, when acetylene black was used as conductive addition, deterioration of the electrode may cause cathode less conductive while cycling thereby cause capacity loss. Rubino *et al.*¹⁹ also found the capacity fade was attributed to electrode swelling during cycling and the

cell reduced the integrity of the electrical conduction network causing active particles to become isolated.

As shown in Figure 6, the ac impedance of the two different types of composite electrodes was measured at 4.25 V versus Li/Li⁺. The Figure inserted represents the equivalent circuit model for LiMn₂O₄ composite electrode, where R_s is the resistance of solution, R_f and CPE1 (Constant Phase Element) are associated with the SEI (Solid Electrolyte Interface) layer resistance and the associated surface layer capacitance. SEI film is an insulator for electron and a good conductor for lithium ion which can freely insert and deinsert through. It has been reported²⁰ that the SEI film on the cathode is composed of various lithium salts, including lithium carbonate (Li₂CO₃), lithium alkoxides (ROLi), and carboxylic lithium (RCO₂Li). R_{ct} and CPE2 are the charge transfer resistance and corresponding double-layer capacitance, respectively. CPE used in place of capacitor to model the data due to the non-homogeneity of the composite electrode system reflected as depressed semi-circle in the impedance response. Z_w is the Warburg resistance. In high frequency region, the depressed semicircle is considered to reflect the properties of SEI layer. The presence of medium-frequency semicircle can be attributed to R_{ct}. From Figure 6, fitting results were identical to the experimental measurements. The parameters obtained from fitting EIS experimental data are listed in Table 1. The values of the exchange current i₀ are calculated according to i₀ = RT/nFR_{ct} (n=1). The R_{ct} of LiMn₂O₄/ox-MWCNT and LiMn₂O₄/AB electrodes were 34.32 and 53.2 Ω, respectively. This implies that the LiMn₂O₄/ox-MWCNT electrochemical reaction on electrode LiMn₂O₄/ox-MWCNT proceeds easily than that on electrode LiMn₂O₄/AB. The electronic conductivity of ox-MWCNT is 2.85×10² S cm⁻¹, which is two orders of magnitude higher than that of acetylene black (2.18 S cm⁻¹). Moreover, the slope in low-frequency of LiMn₂O₄/ox-MWCNT is higher than LiMn₂O₄/AB, indicating that ox-MWCNT wiring can enhance the electrochemical activity of LiMn₂O₄ more effectively than acetylene black.

The increase in the diameter of the mid-frequency arcs of LiMn₂O₄/AB cathode can be interpreted as an increase in R_{ct} and the increasing difficulty in Li⁺ de-intercalation reactions over time which resulting in incomplete charge of the electrodes and hence the low discharge capacity²¹ (see Figure 5).

At low frequencies of Nyquist plot, electrochemical intercalation process is controlled by the semi-infinite diffusion. Apparent diffusion coefficients of Li⁺ ion can be calculated according to the following equation.^{22,23}

$$\sigma = \frac{RT}{n^2 F^2 A \sqrt{2}} \left(\frac{1}{C_L D_L^{0.5}} \right) \quad (1)$$

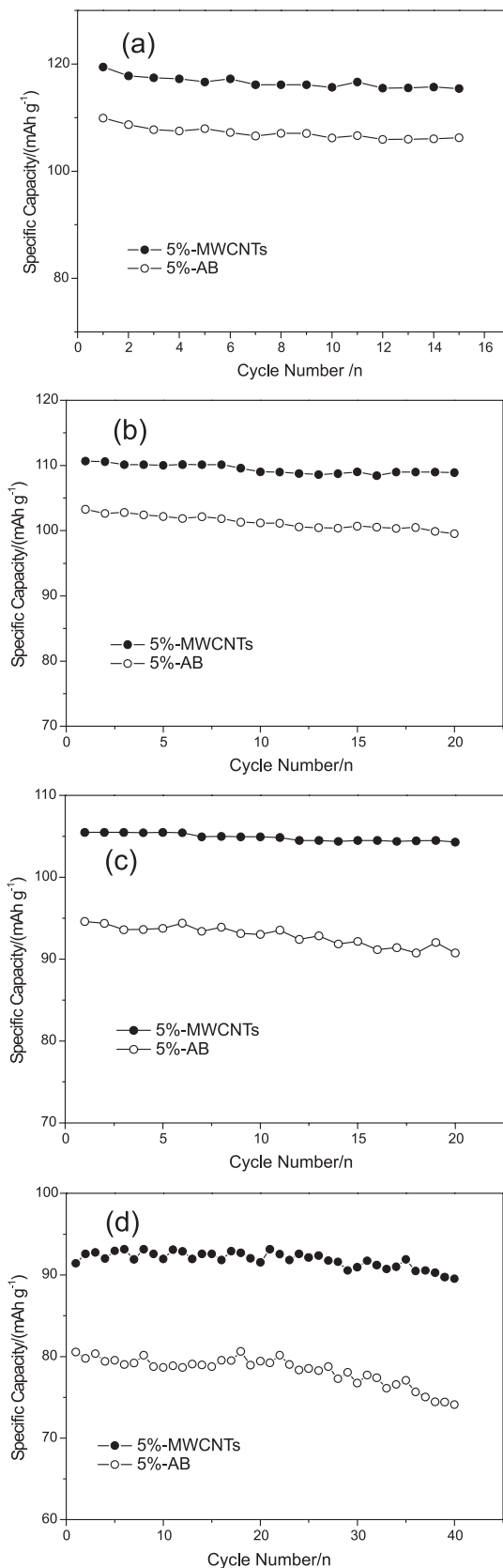
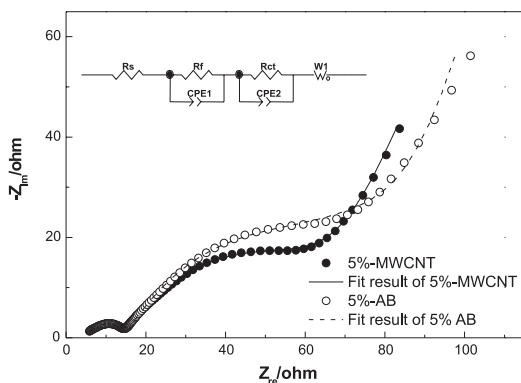


Figure 5. Plots of cycling performance of composite electrodes with ox-MWCNT or acetylene black with the same content (5 wt.%) at different rates (a) 0.1C, (b) 0.5C, (c) 1C and (d) 2C.

Table 1. Equivalent circuit parameters obtained from fitting EIS experimental data of composite cathode with 5 wt.% ox-MWCNTs or acetylene black

	$R_s/(\Omega)$	CPE2-T(10^{-3})	CPE2-P	$R_{ct}/(\Omega)$	$i_0/(\mu\text{A})$
$\text{LiMn}_2\text{O}_4/\text{ox-MWCNT}$	4.85	12.252	0.71388	34.32	0.748
$\text{LiMn}_2\text{O}_4/\text{AB}$	4.789	10.085	0.62255	53.2	0.483

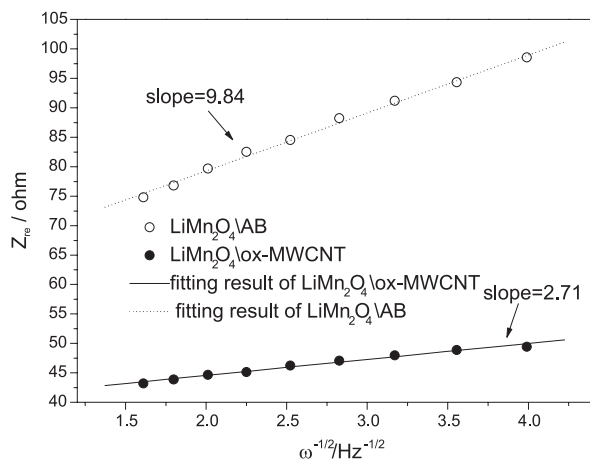
T and P are the constant phase parameters of the equation $Z=1/[T(i\omega)^P]$.

**Figure 6.** Nyquist plot of LiMn_2O_4 composite electrodes with 5 wt.% ox-MWCNT or acetylene black at room temperature (with equivalent circuit inert).

Where C_{Li} is the concentration of Lithium-ion incorporated inside a electrode, D_{Li} the apparent diffusion coefficient, A the geometrical area of the electrode, n the number of electron transferred, F Faraday's constant, R the gas constant, T the absolute temperature, and ω is the angular frequency. And the ω has a relationship with Z_{re} as equation (2) ²³.

$$Z_{\text{re}} = R_{\omega} + R_{ct} + \sigma\omega^{-1/2} \quad (2)$$

Figure 7 shows the real part of the impedance against $\omega^{-1/2}$ of $\text{LiMn}_2\text{O}_4/\text{ox-MWCNT}$ and $\text{LiMn}_2\text{O}_4/\text{AB}$ electrodes in the low frequency region. The slope designates Warburg

**Figure 7.** Real part of the impedance plotted against $\omega^{-1/2}$ of $\text{LiMn}_2\text{O}_4/\text{ox-MWCNT}$ and $\text{LiMn}_2\text{O}_4/\text{AB}$ electrode in the low frequency region.

factor (σ) as shown in equation (2). A small Warburg factor value indicates high diffusion which means high utilization of active material. The diffusion coefficient of lithium ion was calculated based on equations (1) and (2). The D_{Li} of $\text{LiMn}_2\text{O}_4/\text{ox-MWCNT}$ and $\text{LiMn}_2\text{O}_4/\text{AB}$ electrodes were $7.4 \times 10^{-11} \text{ cm}^2 \text{ s}^{-1}$ and $2.9 \times 10^{-12} \text{ cm}^2 \text{ s}^{-1}$, respectively. Dominko *et al.*^{24,25} suggested that the electrochemistry reactions essentially depend on electronic conducting, and the process of lithium ions insertion-deinsertion is accompanied by electron removal simultaneously. Here, the diffusion of lithium ions in the solid state was improved because ox-MWCNT was metallic conducting compared AB. In addition, the formation of the conductive network by ox-MWCNT wiring can improve electron transport and electrochemical activity of cathode materials.

Conclusion

The comparative investigation on the composite cathode of LiMn_2O_4 with the addition of acetylene black and ox-MWCNT revealed that ox-MWCNT increased rate capacity and cycling efficiency remarkably. The electron transport and electrochemical activity were improved effectively by the web wiring structure. Fitting results of EIS experiment showed that R_{ct} of $\text{LiMn}_2\text{O}_4/\text{ox-MWCNT}$ and $\text{LiMn}_2\text{O}_4/\text{AB}$ were 34.32 and 53.2 Ω , respectively. It is due to the formation of a three-dimensional network wiring by ox-MWCNT, which can increase contact area of cathode active materials and reduce the R_{ct} remarkably. Overall, the research is of potential interest to application of ox-MWCNT as a new conducting additive to replace acetylene black and other carbon blacks in the cathode preparation and development high-power lithium rechargeable batteries.

Acknowledgments

Financial support from China Natural Science Foundation (Key Project No.:50542004) is greatly appreciated.

References

1. Sigala, C.; Guyomard, D.; Vebara, A.; Piffard, Y.; Tourmoux, M.; *Solid State Ionics* **1995**, *81*, 167.
2. Wu, Y.-P.; Wan, C.; Jiang, C.; Fang, S.-B.; *Lithium Ion Secondary Batteries*, Chemical Industry Press: Beijing, 2002.

3. Song, D.; Ikuta, H.; Uchida, T.; Wakihara, M.; *Solid State Ionics* **1999**, *117*, 151.
4. Tarascon, J.-M.; Guyomard, D.; *Electrochim. Acta* **1993**, *38*, 1221.
5. Megahed, S.; Scrosati, B.; *J. Power Sources* **1994**, *51*, 79.
6. Tran, N.; Croguennec, L.; Jordy, C.; Biensan, P.; Delmas, C.; *Solid State Ionics* **2005**, *176*, 1539.
7. Jiang, J.; Eberman, K.-W.; Krause, L.-J.; Dahn, J.-R.; *J. Electrochem Soc* **2005**, *152*, A566.
8. Suresh, P.; Shukla, A.-K.; Munichandraiah, N.; *Electrochem Solid-State Lett.* **2005**, *8*, A263.
9. Indrajeet, V.-T.; Vipul, M.; John, N.-H.; Wheeler, D.-R.; *J. Power Sources* **2006**, *162*, 673.
10. Son, J.-T.; Kim, H.-G.; Park, Y.-J.; *Electrochim. Acta* **2004**, *50*, 453.
11. Yang, D.-J.; Wang, S. G.; Zhang, Q.; *Phys. Lett.* **2004**, *207*, A329.
12. Thess, A.; Lee, R.; Nikolaev, P.; *Science* **1996**, *273*, 483.
13. Chen, J.-J.; Whittingham, M.-S.; *Electrochem. Commun.* **2006**, *8*, 855.
14. Thackeray, M.-M.; Kock, A.-de.; Rossouw, M.-H.; Liles, D.; Bittihm, R.; Hodge, D.; *J. Electrochem. Soc.* **1992**, *139*, 363.
15. Kuznetsova, A.; Mawhinney, D.-B.; Naumenko, V.; Yates Jr, J.-T.; Liu, J.; Smalley, R.-E.; *J.Chem.Phys.Lett.* **2000**, *321*, 292.
16. Son J.-T.; Kim H.-G.; Park, Y.-J.; *Electrochim. Acta* **2004**, *50*, 453.
17. Mukai, S.-R.; Hasegawa, T.; Takagi, M.; Tamon, H.; *Carbon* **2004**, *42*, 837.
18. Wang, C.-W.; Cook, K.; Sastry, A.; *J. Electrochem. Soc.* **2001**, *150*, A385.
19. Rubino, R.-S.; Gan, H.; Takeuchi, E.-S.; *J. Electrochem. Soc.* **2001**, *148*, A1029.
20. Matsuo, Y.; Kostecki, R.; McLarnon, F.; *J. Electrochem. Soc.* **2001**, *148*, A687
21. Liu, Z.-L.; Lee, J.-Y.; Lindner, H.-J.; *J. Power Sources* **2001**, *97-98*, 361
22. Ong, T.-S.; Yang, H.; *Electrochem. Solid-State Lett.* **2001**, *4*, A89.
23. Bard, A.-J.; Faulkner, L.-R.; *Electrochemical Methods*, Wiley: New York, 2001, p. 231.
24. Dominko, R.; Gaberscek, M.; Drogenik, J.; Bele, M.; Pejovnik, S.; Jamnik, J.; *J. Power Sources* **2003**, *770*, 119.
25. Dominko, R.; Gaberscek, M.; Drogenik, J.; Bele, M.; Pejovnik, S.; *Electrochem. Solid-State Lett.* **2001**, *4*, A187.

Received: July 12, 2007

Web Release Date: July 11, 2008